POAC'17
Busan, KOREA

Proceedings of the 24th International Conference on
Port and Ocean Engineering under Arctic Conditions
June 11-16, 2017, Busan, Korea

The Entrainment and Migration of Crude Oil in Sea Ice, the Use of Vegetable Oil as a Substitute, and Other Lessons from Laboratory Experiments

Megan O'Sadnick[1], Chris Petrich[1], Nga Dang Phuong[1]
[1] Northern Research Institute (Norut) Narvik, Narvik, Norway

ABSTRACT

Understanding the interaction between oil and sea ice is essential in the development of oil spill detection and response technology in the Arctic. Laboratory experiments were performed to examine oil migration in sea ice during the cold phase and during warming, and investigate the behavior of different oils in sea ice to identify suitable substitute oils for crude oil. Vegetable oil and Troll B crude oil were injected underneath laboratory-grown sea ice with oil lenses either 1 cm or 3 cm in thickness. Results show similar behavior of vegetable oil and crude oil in sea ice both shortly after oil injection and during the warm phase. Further, results are independent of lens thickness. The implications of this result are discussed. In addition, the impact of cylindrical confinement of ice is shown on crystal and brine channel structure, and the energy balance of the tank are discussed.

KEY WORDS: Sea ice; Oil; Microstructure

INTRODUCTION

Research into the interaction between crude oil and sea ice began in earnest in the 1970s with both large scale field studies designed to gained a stronger overall understanding of the topic (NORCOR, 1975; Martin, 1979; Deslauriers, 1978) and smaller scale laboratory experiments which focused on specific aspects of the interaction between oil and sea ice (Keevil and Ramseier, 1975; Mackay et al., 1976) Since that time, research into the oil and ice has expanded with an increasing number of studies focused on the microscale interaction of oil and sea ice including the influence of pore structure on the rise of oil through ice and the associated parameters that may impact this process (Karlsson et al, 2011; Petrich et al., 2013; Maus et al., 2015; Salomon et al., 2017).

Due to current environmental regulations, it is difficult to perform experiments in the field examining the interaction between crude oil and sea ice. This concern provides the first objective for our experiment:

1) *The comparison of crude oil to vegetable oil* to determine the suitability of the latter as a replacement in experiments.

The three additional objectives of this study are:

2) *The examination of the parameter space including the influence of lens thickness without added hydrostatic pressure from encapsulation and time elapsed on the migration of oil upward.* To ensure only lens thickness influences movement of oil upwards, ice melt is initiated before an ice cap can form beneath the lens. The pressure potentially created as ice encapsulates the oil lens is therefore prevented simplifying analysis of results from lenses of differing thicknesses.
3) *The influence of cardboard cylinders on ice growth and oil migration.* Use of cylinders allows for the easy containment of oil lenses and ability to control lens diameter and thickness independent of under-ice topography. However, ice structure and brine channels in cylinders have not yet been characterized.
4) *The quantification of the energy balance of ice tanks.* Quantifying growth conditions in ice tanks allows for more accurate and detailed comparisons to be made across experiments, in both the laboratory and field, and enhance our ability to alter conditions to suit the needs of an experiment.

METHODS

To prepare samples of artificial sea ice, two tanks with slanted walls, each having the dimensions of 0.50 x 0.50 x 0.50 m, were first filled with a mixture of fresh water and Blue Treasure Synthetic Salt to a level of 0.41 m (Salomon et al., 2016). Starting salinity in both tanks was 32.9 ppt. A probe measuring temperatures in 1 cm vertical intervals was installed in each tank. Thermocouple wires ran horizontally along the width of the tank in an effort to decrease heat conduction and the buildup of ice at the temperature probe (Figure 1b). Cardboard tubes to confine oil during injection were suspended from metal rods above the water surface and reached to a depth of about 0.16 m below the water surface (Figure 1a & 1b).

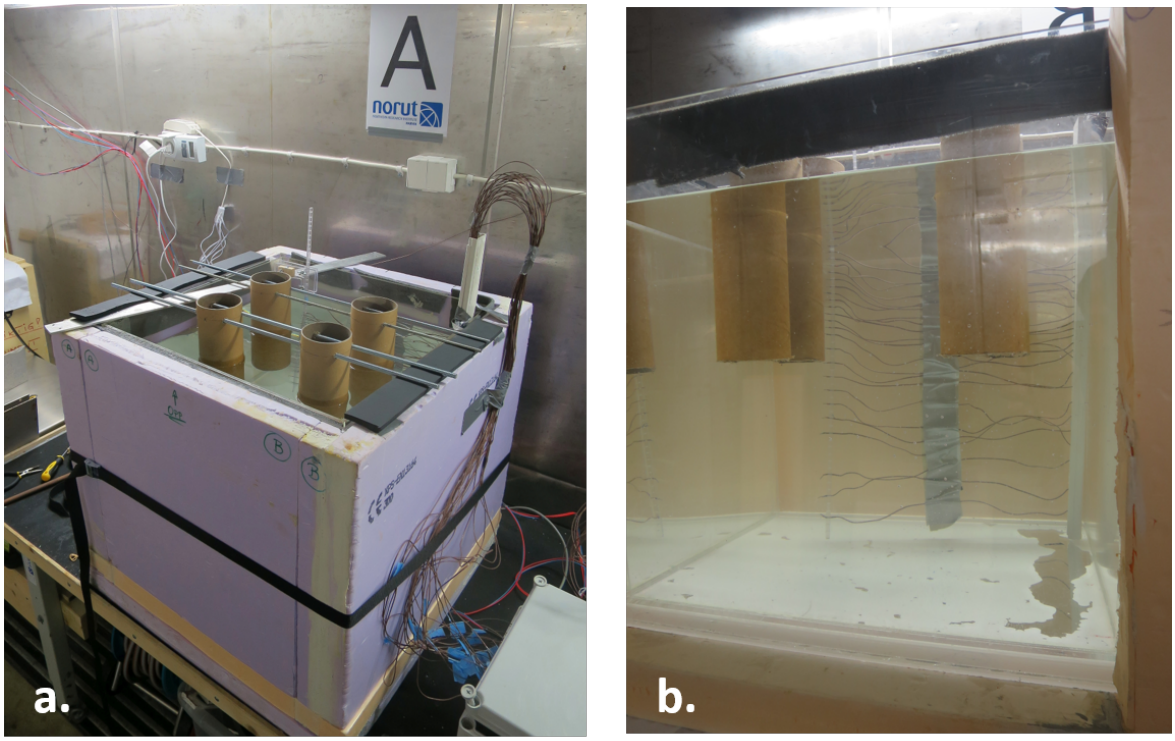

Figure 1. Experimental setup a) Overview of tank setup showing placement of thermocouples and cardboard tubes for oil injection; b) View of tubes and thermocouples from below the water surface.

Once setup was complete, the ambient temperature in the cold room was lowered to 0 °C to allow for the even cooling of the salt water prior to onset of ice formation. After two days, the ambient temperature was set to -15 °C to initiate ice growth. Due to the slanted design of the tank, the ice grew free-floating and developed a natural freeboard.

Once the ice reached a thickness of approximate 0.10 m, oil was injected. In Tank A, a mixture of rapeseed oil dyed with Sudan III at a concentration of 0.03% (w/w) was used. Of a range of store-brand vegetable oils tested (olive, sunflower, soybean, rapeseed, and fry oil),rapeseed oil was chosen as it was the oil with the lowest pour point of around -15 °C. Sudan III is a lysochrome, i.e, an oil soluble dye used to improve visualization of oil movement in the ice. In Tank B, North Sea crude oil from the Troll B field was used. Troll B is a sweet, naphthenic crude oil with a low pour point. A syringe having volume of 60 ml and a teflon tube were used to inject the oil. Care was taken to avoid the presence of air bubbles in the tube and subsequently the oil lens. Given the presence of cardboard tubes, injection was easy to control with spillage outside of the tubes being negligible. Four oil lenses were injected into each tank, with two lenses having a thickness of approximately 0.01 m and the other two lenses a thickness of 0.03 m - volumes of $2.8 * 10^{-5}$ m^3 and $8.5 * 10^{-5}$ m^3, respectively.

After four hours, one lens of each thickness was removed from both tanks using a saw to cut around the cardboard tubes. Cores were held vertically upright to prevent oil moving higher up into the ice than it had already. Since the oil lenses were not overgrown yet, most of the oil held in the lens was lost. Immediately after core removal, dry ice was packed upward into the cardboard tube to cool ice and oil and retain oil in the pore space (and potentially at the lower ice interface). The samples were quickly transported to a -80 °C freezer to stop any further movement of oil and prepare for future analysis. Samples were stored vertically. As a substantial volume of ice was removed from the tanks during this process, additional ice was placed into the tanks to ensure freeboard, similar to before removal, was maintained.

To examine the migration of oil upwards without the potential impact of pressure arising from the encapsulation of the oil lens, melt was initiated immediately after ice removal by increasing the air temperature to -2 °C. All four remaining cores were removed at the first observed surfacing of oil, which occurred about 30 hours after oil injection. In an attempt to preserve the location of oil in brine channels, cores were laid horizontally immediately after removal and dry ice was packed into the bottom and top of the cardboard tube. All samples were next placed in the -80 °C freezer horizontally.

Cores were stored in the -80 °C freezer between 8 and 17 days before being sectioned and photographed in the cold room at -15 °C to document any migration of oil upwards. Careful sectioning and realignment enabled us to take both vertical and horizontal sections of the ice cores. Horizontal sections between 5 and 20 mm thickness were melted to measure oil concentration and salinity. To measure the concentration of vegetable oil in cores removed from Tank A heptane was next added to the sample in a beaker of known weight in an amount at least equal in volume to the brine and oil mixture. Through vigorous mixing, the oil was extracted into heptane. Once a clear separation of heptane and brine appeared, brine was separated with a pipette. The remaining mixture of oil and heptane was left for heptane to evaporate, leaving behind only vegetable oil. The beaker was again weighed and the difference taken to be the mass of oil present in that slice of ice.

For melted crude oil samples, the oil was extracted with heptane. The exact amount of heptane used was recorded. The oil concentration in the heptane was then measured using a UV-

fluorescence meter TD500^{TM} (Turner Designs Hydrocarbon Instruments, Inc) which was calibrated to the crude oil prior to analyses according to standard procedures.

For both vegetable oil and crude oil samples, measurements of conductivity were taken on the remaining brine to determine sea ice bulk salinity. Temperature and salinity measurements of the ice were used to calculate brine volume fraction using equations derived from Cox and Weeks (1983).

RESULTS

In Figure 2, the evolution of ice and water temperature during the ice growth phase is presented. The freeze-in of each thermocouple is represented as a clear deviation from the average sea water temperature located around -2 °C. This thus provides a view of the rate of ice growth in each tank.

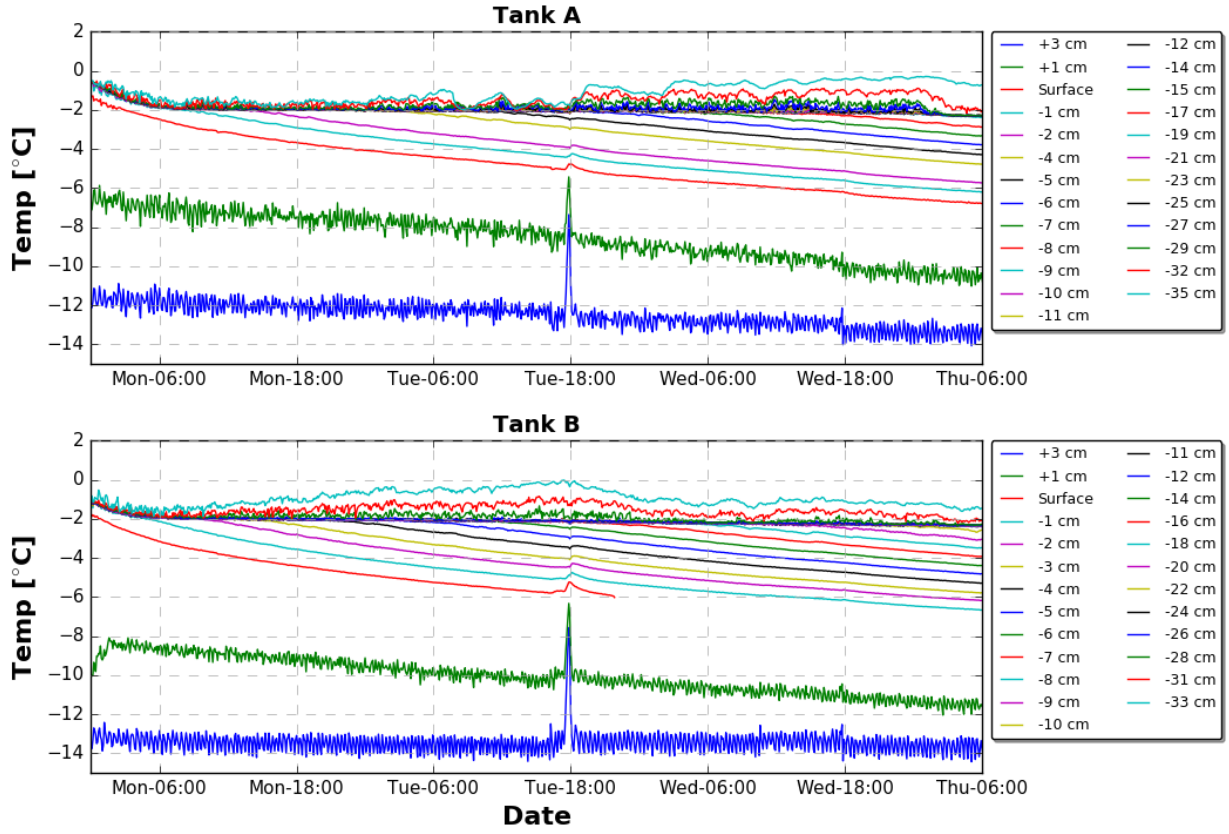

Figure 2. Evolution of temperature in Tanks A and B.

To examine the geometry of brine channels and the path oil traveled upwards, vertical thick sections were photographed of all cores (Figure 3). The vertical section was cut near brine channels visible in the bottom of the core. The temperature, salinity, and brine volume fraction profiles are presented in Figure 4 along with measurements of oil concentration.

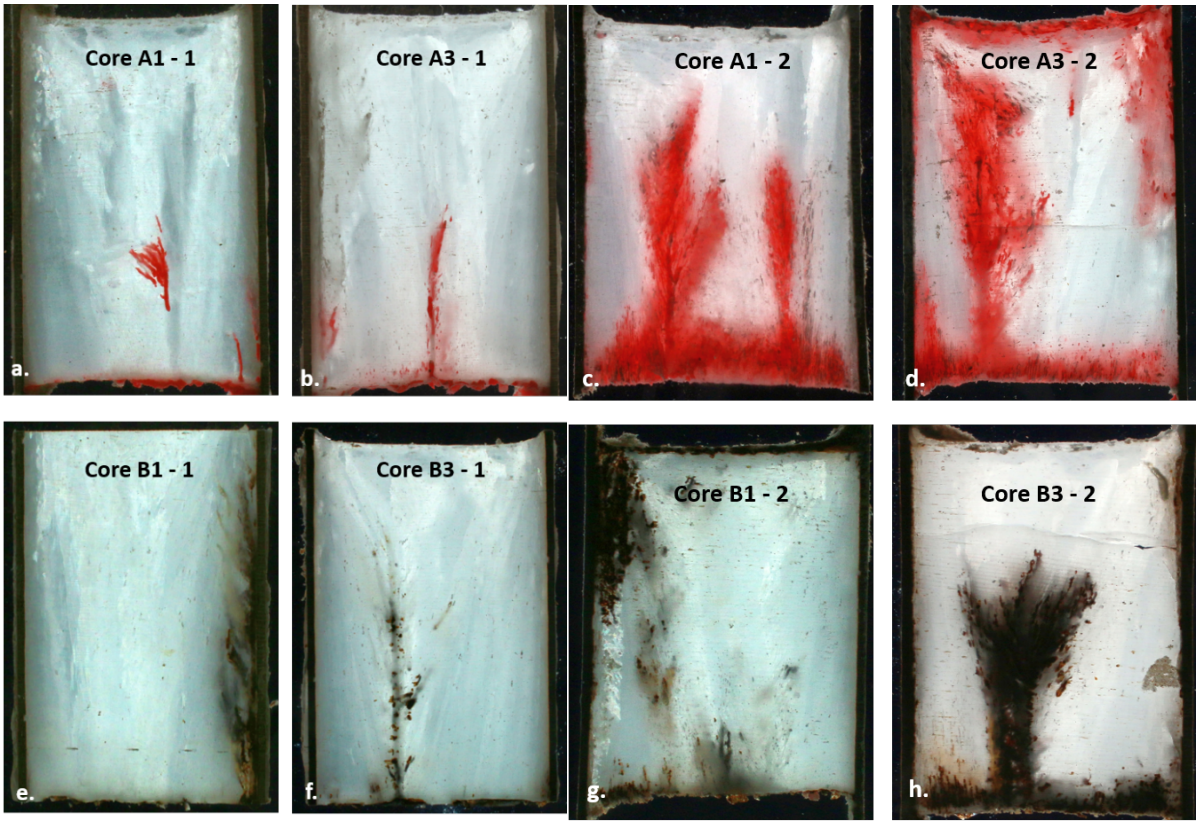

Figure 3. Vertical thick sections (approx. 10 mm thick) obtained from each core removed. (a,b,c,d) dyed vegetable oil and (e,f,g,h) crude oil, (a,c,e,g) oil lens thickness 0.01 m and (b,d,f,h) 0.03 m, and (a,b,e,f) cold ice after 4 hours, and (c,d,g,h) warm ice after 30 hours. The lower part of the channel in (a) was outside of the plane of the thick section.

Ice Properties

Four hours after injection, ice in Tank B was approximately 0.5 °C colder than in Tank A (Figure 2). This is likely due to circulation patterns in the cold room with Tank B being closer to the air outlet and thus exposed to drafts that led to more convective heat loss. As a result, ice thickness was slightly greater and porosity lower throughout the ice in Tank B in comparison to Tank A. However, bulk salinity was relatively consistent between the two tanks (Figure 4). After 30 hours of warming, ice temperature had evolved to be homogenous in both ice tanks. As expected, salinity generally decreased as brine drained resulting in an increased salinity only in the bottom 0.01 – 0.03 m. Porosity was below 20% in the cold ice and increased above 20% throughout the ice during melt (Figure 4). Inside the cardboard tubes, the lamellar structure at the ice–water interface and the crystal structure in horizontal sections (Figure 5) showed axial-symmetric alignment, i.e. horizontal *c*-axes aligned radially from the center.

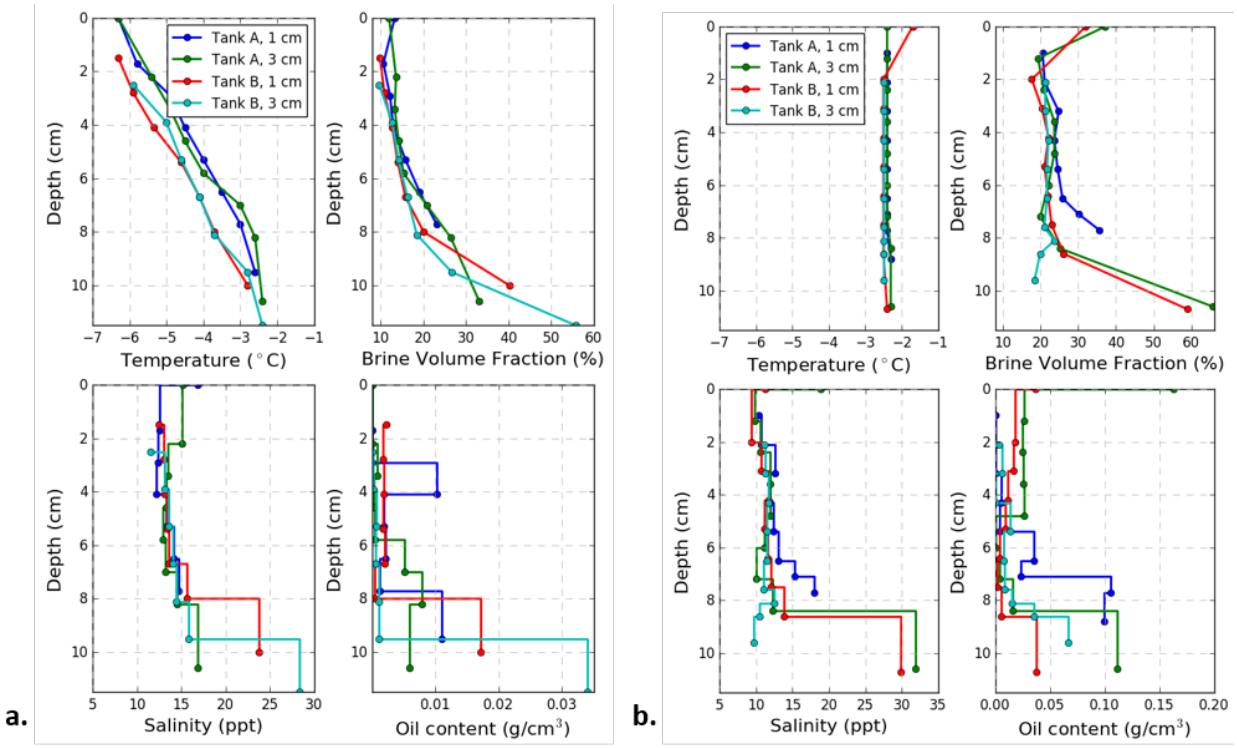

Figure 4. Profiles of ice properties and oil concentration from cores removed at 4 hours (a) and 30 hours (b). Note the different scales of oil content.

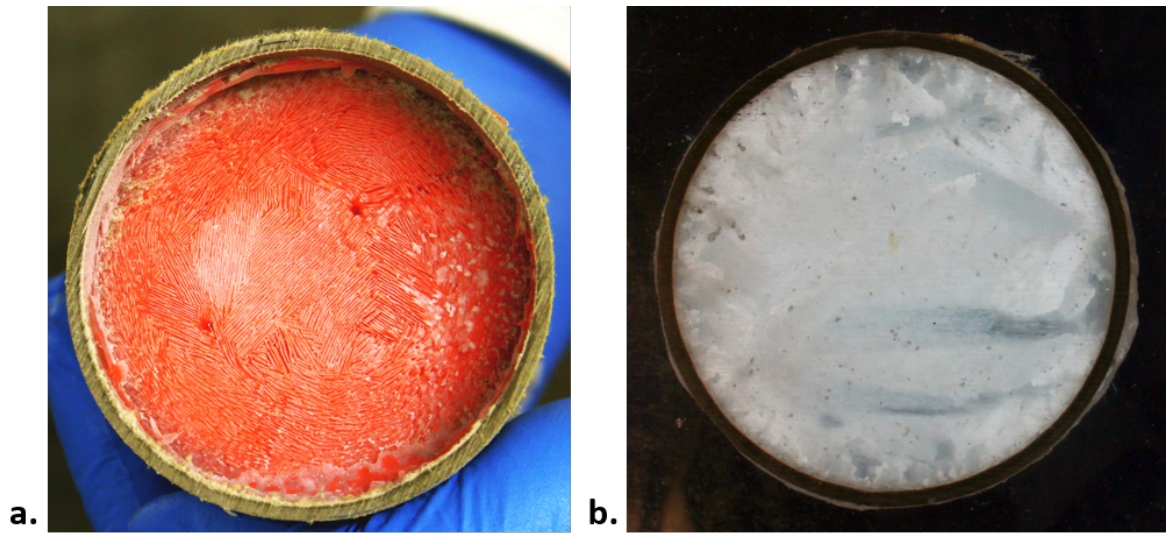

Figure 5. a) Lamellae structure of Core A1-2 at ice-water interface. Note the circular pattern of lamellae around the perimeter, and two brine channels (circular holes). b) Horizontal thick section showing crystal structure of Core B1-1, through cross-polarized filters, at approximately 6 cm depth.

Migration during the initial 4 hours

Figures 3a, 3b, 3e, and 3f as well as plots of oil concentration in Figure 4a, reveal migration only 4 hours after injection in all cores. In one of the two crude oil samples (Core B1-1, Figure

3f), oil travelled up only along the cardboard tube to reach the surface. It is presumed that this extreme migration is due to a weak bond or high porosity at the interface between ice and the cardboard. In the remaining three samples, migration occurred primarily through a brine channel located in the center of the core.

Of all samples taken in cold ice, one vegetable oil sample showed particularly pronounced top-heavy fanning of an oil-filled channel (Figure 3a, Core A1-1). This fanning of the brine channel is reflected in a peak of oil concentration 0.04 to 0.05 m below the ice–air interface (Figure 4a, Tank A 1 cm). Neither such peak (Figure 4a), nor such pronounced fanning (Figure 3) have been found at the upper ends of the channels in either Core B3 - 1 and Core A3-1. In fact, both cores show a trend toward decreasing oil content with distance above the oil lens.

The amount of oil entrained into the skeletal layer is small and limited to the bottom-most millimeters in Cores 3A-1 and 3B-1 (Figure 3). Entrainment appears to be in droplet form and more concentrated around the brine channel. Measurements of these small amounts of entrainment into the skeletal layer are difficult to perform quantitatively since the separation between oil lens and skeletal layer may not have been clean and some oil from the lens may have held on to the interface before it got immobilized by dry ice. As a result, all cores have a measureable amount oil at this depth despite little visual evidence inside the lamellar layer.

Migration over 30 hours

The remaining cores were all removed upon the first sight of oil surfacing. Vertical thick sections show more diffuse oil distribution compared to the distinct channel features in cold ice (Figure 3). Surfacing of oil occurred in Cores A3-2 (vegetable oil) and B1-2 (crude oil) 30 hours after injection. In both cores, the migration reaching the surface seemed to have occurred along the interface between the ice and cardboard tube. In Core A3-2, a large oil-filled brine channel was also present at the center of the core. The combined contributions may explain the high oil content from the surface down to 0.05 m depth (Figure 4b, Tank A, 3 cm).

In Cores B3-2 and A1-2, migration of oil occurred primarily through large brine channels close to the center of the core (Figure 3c, h). Two oil-filled channels developed in Core A1-2, neither leading to the surface but with one branching substantially outward toward the top. In Core B3-2, this branching occurred to the greatest degree of any of the cores. However, the oil profile in Figure 4b shows that the oil concentration decreased monotonously with distance from the oil lens, indicating that the increase in penetrated horizontal cross-sectional ice area was accompanied by a decrease of oil concentration within that penetrated cross-section.

Evident in all warm cores is entrainment of oil into the skeletal layer between 10 and 20 mm. Oil appears to have travelled the greatest distance in Core A1-2. This behavior is seen in measurements of oil concentration with Core A1-2 having 0.05-0.10 g/cm^3 in the 20 mm above the oil lens (i.e., from 0.07-0.09 m), equivalent to 10% oil by volume. In the other cores, high oil concentration in the skeletal layer is only seen in the bottom 0.01 m.

DISCUSSION

Comparing Vegetable Oil to Crude Oil

In comparing the behavior of vegetable oil to crude oil over 4 hours and 30 hours, many similarities are apparent between the oils. After 4 hours, little to no infiltration of the skeletal layer occurred in samples containing both kinds of oil (Figure 3). The migration of oil upwards was largely dependent on the presence of a main brine channel in the center of the core. When present, oil in all cores travelled up to 0.04 to 0.03 m below the ice surface. While a higher concentration of oil was present in cores with vegetable oil, this may be due to the branching

away from the main brine channel observed, particularly apparent in Core A1-1. Possibly the most plausible explanation for this was that the brine channel in Core A1-1 fanned out more than in other cores. While no measurements of viscosity were obtained on vegetable or crude oil samples at relevant temperatures, at room temperature, the viscosity of vegetable oil is about 10 times higher than the viscosity of Troll B crude oil. Measurements of the respective interface tension are not available. One could surmise from our findings however, that the vegetable oil did not flow much easier through cold ice than crude oil. Examination of cores gathered after 30 hours provides some insight into these findings.

Cores A3-2 and B1-2 both had oil surface due to oil traveling up along the side of the core (Figure 3). Cores A1-2 and B3-2 however, had the majority of oil migration occur through brine channels located near to the center of the core. Oil lens thickness did differ between these two cores, however the height to which oil travelled upward is comparable between the two cores. The largest difference in oil concentration was observed near the bottom of the core, 0.08 to 0.10 m from the top. In Core A1-2, oil concentration reached over 0.10 g/cm^3 due to the high level of oil infiltration into the skeletal layer. From these results, it appears the vegetable oil and crude oil exhibit similar behavior in ice when large brine channels exist. Where differences occur and where further investigation is required is the ability of both to travel into the skeletal layer as well as into narrower channels that branch from the main brine channel. The low entrainment depth is particularly noteworthy in cold ice compared with expectations from earlier experiments and field work (Karlsson et al. 2011; Petrich et al. 2013). Differences between those experiments and the experiments reported here are the absence of overgrowth of the oil lens. It had been hypothesized that the overgrown ice cap pressurizes the oil due to buoyancy (Martin, 1979), potentially explaining the missing observation of entrainment.

Impact of Lens Thickness, Time Elapsed, and Oil Movement

In examining cores to determine the impact of lens thickness and time elapsed, perhaps the most evident differences occur in the skeletal layer. The skeletal layer is composed of freshly formed platelets slowly protruding themselves into a thin layer of supercooled sea water below. It is highly porous and in both this and previous laboratory experiments performed at Norut Narvik, has been found to be typically 0.01m thick in cold ice. Therefore, unlike brine channels, the structure of the skeletal layer is relatively consistent across experiments and tanks. Examining entrainment of the skeletal layer as a potential function of lens thickness, no strong pattern emerges. At 4 hours, all cores of both differing oil type and lens thickness display little to no oil in the skeletal layer. It is the two cores with 0.01 m lens thickness that held the highest concentration of oil, between 0.01 and 0.02 g/cm^3 – an amount lower by an order of magnitude from cores collected at 30 hours. In cores with a lens of 0.03 m, small droplets of oil are visible particularly centered nearer to the brine channel. While it was not possible to quantify that oil with our methods, it suggests that lens thickness may impact how quickly oil settles into the skeletal layer initially. Closer examination with techniques such as micro tomography (uCT) may shed light on the entrainment process (Salomon et al., 2016; 2017).

Despite little movement into the skeletal layer, both vegetable oil and crude oil migrated through established brine channels after only four hours. The length of these channels varied from approximately 0.04 m to 0.07 m. This finding compares nicely to that of the 1975 NORCOR crude oil in ice experiment where oil spilled beneath cold natural ice in late fall also migrated on average between 0.04 – 0.06 m up brine channels. A greater amount of oil was observed in the skeletal layer during the NORCOR experiment, however, this may possibly be related to the encapsulation of the oil lens that occurred.

In cores removed after 30 hours, no dominant pattern emerged between cores of differing lens thickness. The largest entrainment depth was observed in vegetable oil of 0.01 m lens thickness, essentially the one expected to develop the least entrainment. Reduced oil entrainment may be attributed to the presence of brine channels for oil to travel upward. The two cores with the greatest concentration of oil in the skeletal layer had little to no movement of oil up along the cardboard tube. It is therefore surmised that the channels that formed at the cardboard tube acted to drain oil from the lens and reduce hydrostatic pressure before oil was able to fully entrain the skeletal layer.

Given the difference in oil movement above the skeletal layer up into channels, it is harder to draw conclusions on the impact of lens thickness on oil movement through channels and branches leading away from the main channel. Core A3-2 displayed a large broad channel with oil branching from the main trunk in addition to oil between the core and cardboard. In contrast, Core B1-2 showed greater migration of oil upwards than Core B3-2 due to a brine channel along the edge of the core. Oil is also visible within the core, possibly from movement up other small channels. In the sample having a 0.03 m crude oil lens, oil did not reach the surface but did branch outward extensively. Thus, from these findings, it appears that lens thickness did not play a dominant role in the migration of oil upward.

Further Lessons for Future Experiments

Cardboard Cylinders for Oil Containment

The use of cardboard cylinders to contain oil has its downfalls as displayed particularly in Figure 3d, 3e, and 3g. In these cores, oil traveled primarily up through the pore space at the ice-cardboard interface, the result likely of a weak bond between the two. In addition, a clear pattern arose in the ice crystal structure and lamellae somewhat circular in shape and reminiscent of tree rings (Figure 5). This pattern is believed to be caused by convection patterns formed within the tube. Convection has been shown to drive crystal alignment, including at the scale of 10-cm relevant for this experiment, and it is the reason for the development of brine channels (Langhorne and Robinson, 1986; Worster 1997; Petrich et al. 2007). As the development of brine channels in sea ice is often unpredictable, this finding may aid in the design of future experiments involving brine channels. Measures to avoid migration along the cardboard-ice interface are needed however. One simple solution is to prevent contact between cardboard and oil entirely by placing small pieces of insulation at the surface. This will create thicker ice at the walls of the cardboard thus creating a small ‘pocket’ at the center of the core.

The Balance of Heat in Ice Tanks

Ice, air and water temperature data from the temperature probe were evaluated to examine the energy balance of both tanks during the ice growth phase. Ice growth took place in darkness, reducing the energy balance equation to

$$\dot{Q}_H = \dot{Q}_C + \dot{Q}_I + \dot{Q}_L, \quad (1)$$

where $\dot{Q}_H$ is the rate of change of enthalpy of the sea ice and water, $\dot{Q}_C$ is the conductive heat flow across the ice–air interface, $\dot{Q}_I$ is the sensible heat input into the system at the bottom of the tank, and $\dot{Q}_L$ is the heat loss through the sides of the tank and at the bottom. The heat loss terms are calculated as the residual of Eq. (1), all other terms are calculated or known.

In Figure 6a, ice temperature is used to model depth-average brine salinity within the ice, depth-averaged porosity, and enthalpy of the tank. Results for porosity show higher porosity in Tank A than in Tank B, consistent with Figure 4a. Also, the enthalpy stored in Tank B was larger than in Tank A.

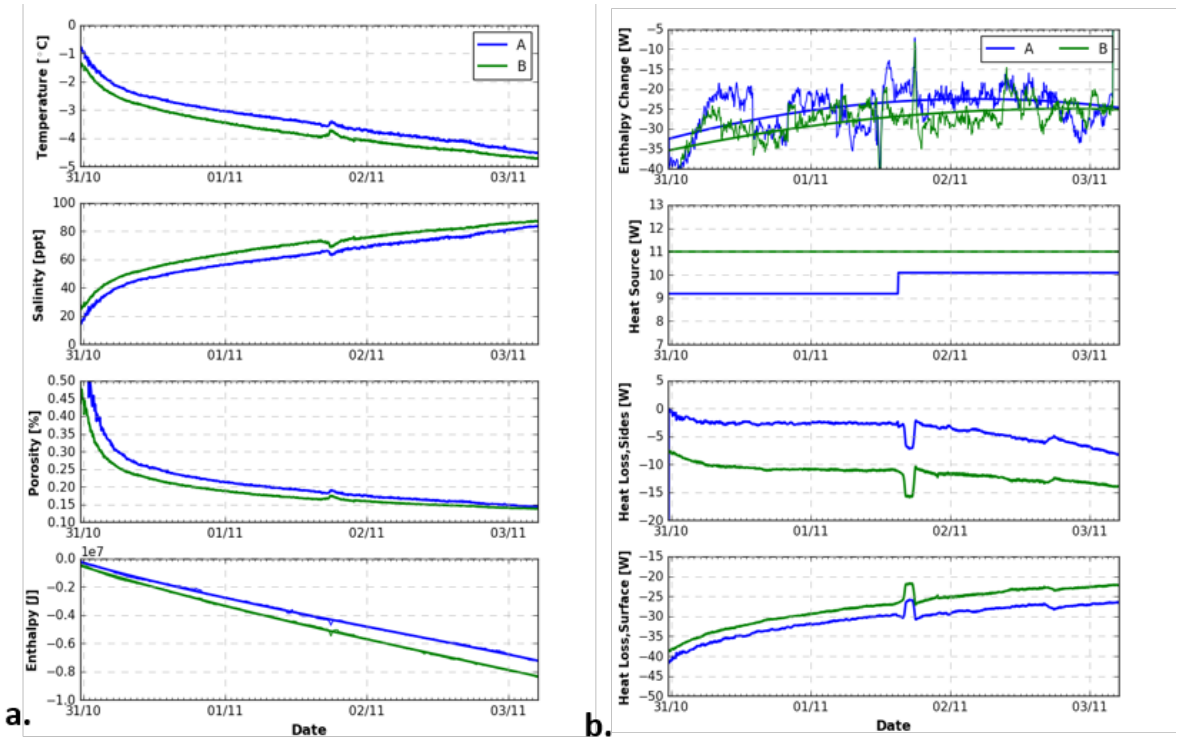

Figure 6. a) Calculation of enthalpy from modeled values of porosity and salinity derived from measurements of temperature; b) Heat balance with Tanks A and B. In (b), the rate of enthalpy change was calculated over 5 minute intervals with a third-order polynomial fit applied over measurements every 6 hours. The cross sectional area of the tank was 0.25 m^2, suggesting initial conductive heat loss rates through the surface of up to 160 W/m^2.

Figure 6b compares the derived heat flow rates. At the beginning of the experiment, the energy balance is dominated by the conductive heat flow and enthalpy change, indicating that ice formation is dominated by 1-dimensional heat loss to the surface. However, the heat loss to the sides and bottom increases in magnitude toward the end of the ice growth period while the surface heat flow decreases in response to thickening ice. The former is likely due to an increase in the difference between tank and air temperature which will continue to grow in magnitude as ice thickens. In Tank A, the magnitude of the surface flow is shown to be consistently larger than in Tank B due to ice being 0.01 m less in thickness. The difference in thickness is further reflected in measurements of enthalpy and enthalpy change. Values represent enthalpy in both ice and water and were derived using values of average temperature found in both. The greater the magnitude of enthalpy change, the greater amount of ice present in the system. The heat loss to sides and bottom of the system are consistently higher in Tank B than in Tank A, which is ascribed primarily to the placement of Tank B in the direct draft of the cooling system.

In the second panel of Figure 6b, heat input is presented. While both tanks were set up similarly, a higher heat flux was initially applied to Tank B in an effort to counter the greater amount of heat loss. In Tank A, heat input was increased midway through the ice growth process due to the formation of platelet ice along the sides of the tank and at the ice–water interface. This action was helpful in avoiding platelet growth and did not impact total ice growth substantially. This finding is useful in designing future experiments where one aims for consistent ice growth, a flat ice/water interface, and little to no platelet formation.

Heat flux through the side was determined as the residual of the other three terms. This is the flux through the four sides of the tank and the bottom, each having approximately 0.05 m of insulation. As time progressed, ice thickened, and average temperature in the two tanks dropped, heat flux through the sides increased in magnitude. The difference between Tank A and Tank B is particularly evident in this plot with Tank B having often greater than double the flux through the tank sides than in Tank A. However, distributing the heat flow through the sides between four or five sides, it is evident that the sides were insulated and ice growth is still dominated by flux through the surface in both tanks. The flux through the surface was often more than ten times greater than flux through any one side of the respective tank.

CONCLUSIONS

To develop a complete understanding of the migration of oil through sea ice it is at times advantageous to downscale experiments to constrain the impact of various parameters and focus on specific aspects of the process. In doing so, useful data can be collected while also often saving on both cost and time. Using this approach, we were able to reach the following conclusions that both add to current knowledge of oil in sea ice and will assist in the design of future laboratory experiments.

1) Vegetable oil that is known to still flow at -15 °C displays similarities to Troll B crude oil in its movement through brine channels and the rate of migration to the surface. Hence, vegetable oil can be a suitable alternative to study the general process of oil migration through sea ice. Further studies need to be conducted quantifying the crude oils and circumstances where vegetable oil cannot serve as a substitute.
2) The thickness of the oil lens did not have a noticeable impact on the migration of oil upward in this experiment (comparing 0.01 m with 0.03 m lens thickness under 0.1 m ice). The dominant factor was instead the presence and placement of brine channels. Entrainment in the skeletal layer after four hours was low or nonexistent for lenses of either thickness. Presumably, this was because an ice cap had not yet formed beneath the oil lens, limiting the magnitude of hydrostatic pressure driving oil into the ice.
3) Cardboard cylinders do have an impact on the crystal structure and brine channel morphology of the sea ice formed within due likely to patterns in fluid flow created by the cylinder (cf. Petrich et al., 2007). Such cylinders therefore provide a potential method to generate brine channels above the oil lens for a targeted study. Much care needs to be taken, however, to limit migration at the interface between the cardboard and ice.
4) The heat balance within the tanks shows the greatest amount of heat loss is through the surface with loss through the sides being an order of magnitude lower. Heat flux in to the tank from resistors placed below, assisted in the prevention of platelet formation while not impacting overall ice growth.

ACKNOWLEDGEMENTS

Funding was provided by the Research Council of Norway (RCN) PETROMAKS2 program through project MOSIDEO (project number 243812), RCN Center for Research-Based Innovation (SFI) CIRFA (grant number 237906), and the European Union's Horizon 2020 research and innovation program under grant agreement No 679266 (GRACE). In addition, we would thank Statoil for supplying crude oil from the Troll B field.

REFERENCES

Deslauriers, P.C. (1978). The Bouchard No. 65 Oil Spill in the Ice-Covered Water of Buzzards Bay. *Journal of Petroleum Technology,* pp. 1092- 1100.

Karlsson, J., Petrich, C., & Eicken, H. (2011). Oil entrainment and migration in laboratory-grown saltwater ice. *Proceedings of the 21st International Conference on Port and Ocean Engineering under Arctic Conditions (POAC)*, Montreal, Quebec, Canada, 10–14 July 2011. Paper POAC11-186, 10 pp.

Keevil, B.E., & Ramseier, R.O. (1975). Behavior of Oil Spilled Under Floating Ice. *Conference on Prevention and Control of Oil Pollution*, pp. 497-501.

Langhorne, P. J., & Robinson, W. H. (1986), Alignment of crystals in sea ice due to fluid motion, *Cold Regions Science and Technology*, 12, 197–214.

Mackay, D., Medir, M., & Thornton, D.E. (1976). Interfacial Behavior of Oil Under Ice. *The Canadian Journal of Chemical Engineering*, 54, pp.72-4.

Martin, S. (1979). A Field Study of Brine Drainage and Oil Entrainment in First-Year Sea Ice. *Journal of Glaciology*, 22(88), 473-502.

Maus, S., Becker, J., Leisinger, S., Matzl, M., Schneebeli, M., & Wiegmann, A. (2015). Oil Saturation of the Sea Ice Pore Space. *Proceedings of the 23rd International Conference on Port and Ocean Engineering under Arctic Conditions*, Trondheim, Norway.

NORCOR, (1975). The Interaction of Crude Oil With Arctic Sea Ice. *Beaufort Sea Project, Department of the Environment*

Petrich, C., & Arntsen, M. (2013). Laboratory studies of oil encapsulation under growing sea ice. *Proceedings of the 22nd International Conference on Port and Ocean Engineering under Arctic Conditions (POAC)*, Espoo, Finland, 9–13 June 2013. Paper POAC13-014, 10 pp.

Petrich, C., Karlsson, J., & Eicken, H. (2013). Porosity of growing sea ice and potential for oil entrainment. *Cold Regions Science and Technology*, 87, 27–32, http://dx.doi.org/10.1016/j.coldregions.2012.12.002.

Petrich, C., Langhorne, & Haskell, P.J. (2007). Formation and structure of refrozen cracks in land-fast first-year sea ice, *Journal of Geophysical Research*, 112, C04006, 1–13, http://dx.doi.org/10.1029/2006JC003466.

Salomon, M. L., Maus, S., Arntsen, M., O'Sadnick, M.,Petrich, C., & Wilde, F. (2016). Distribution of oil in sea ice: Laboratory experiments for 3-dimensional micro-CT investigations. Presented at the *2016 Conference of the The International Society of Offshore and Polar Engineers (ISOPE),* Rodos, Greece, 26 June-1 July 2016.

Salomon, M.L., Arntsen, M., Dang, N.P., Maus, S., O'Sadnick, M., Petrich, C., Schneebeli, M., Weise, M. (2017). Experimental and micro-CT study on the oil distribution in laboratory grown sea ice. *Proceedings of the 24th International Conference on Port and Ocean Engineering Under Arctic Conditions*, Busan, Korea,11-16 June 2017.

Worster, M.G. (1997), Convection in mushy layers, *Annual Review of Fluid Mechanics*,

29, 91–122.